

## Theoretical Studies on the Catalytic Oxidation of Carbon Monoxide on Nickel Clusters

A. K. SRIVASTAVA,<sup>†</sup> Isao KOJIMA,<sup>††</sup> and Eizo MIYAZAKI\*

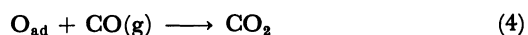
Department of Chemistry, Tokyo Institute of Technology, Ookayama, Meguro-ku, Tokyo 152

(Received April 25, 1986)

Complete neglect of differential overlap (CNDO) molecular orbital calculations using the method of Anno and Sakai for the evaluation of the valence orbital ionization potential (VOIP) were performed with the aim of studying the oxidation of carbon monoxide on nickel clusters. A cluster surface was assumed to be preadsorbed with oxygen and the variation of various bond energies with the approach of a carbon monoxide molecule was studied for different models. Various possibilities for the reaction path are discussed in the light of the theoretical findings and it is suggested that at a low coverage of oxygen the reaction may follow a Langmuir–Hinshelwood path, whereas at a high coverage, an Eley–Rideal path might be more probable.

A catalytic reaction on a solid surface is not simple, but comprises several reaction steps in which a reaction cycle must be formed, starting from an initial chemisorption process of reactants to a closing process by desorbing final products from the surface. Under such requirements for a catalytic reaction, the most stable chemisorbed state among the several possible states is not always the most effective one for completing the catalytic reaction, since this kind of chemisorbed state occasionally remains persistently on the surface without desorbing into the gas phase. The above-mentioned concept should be important for studying, as a whole, a reaction mechanism on heterogeneous catalysts. In order to do so, calculations of all the bond energies as well as the total energies involved in the catalytic cycle are required. In the present paper, we have attempted a new approach to this problem through, as an example, an oxidation reaction of carbon monoxide on a Ni surface using the CNDO molecular-orbital method.

The oxidation of carbon monoxide over active metal catalysts (e.g. Pt, Pd, Rh, Ru, and Ni) has been investigated by numerous workers under well defined conditions with single crystals<sup>1–11)</sup> as well as with polycrystalline surfaces.<sup>12–16)</sup> The individual steps which are possibly involved in the oxidation of carbon monoxide can be given as follows:



A dissociative adsorption of oxygen is well established above 100 K as can be concluded from isotopic exchange experiments<sup>17)</sup> and also from the absence of features in the UPS spectrum that could be assigned to

adsorbed molecules;<sup>18,19)</sup> hence, the reaction steps involving  $\text{O}_{2\text{ad}}$  need not be taken into consideration. Step (3) represents a Langmuir–Hinshelwood path, which predicts a reaction between both the reactants in a chemisorbed state. Steps (4) and (5) represent an Eley–Rideal mechanism in which one of the reactants is in its normal chemisorbed state ( $\text{O}_{\text{ad}}$ ) and the second reacts either through a direct collision from the gas phase or from a weakly held physisorbed or molecular state. At present it is widely believed that the oxidation of CO on noble metal surfaces (such as Pd and Pt) follows a predominantly Langmuir–Hinshelwood type mechanism; evidence for this was earlier obtained from nonstationary studies<sup>2,4,6)</sup> and its dominance has been mainly proposed by recent molecular-beam experiments.<sup>7,8)</sup> However, in addition to these extreme possibilities a precursor mechanism including an Eley–Rideal like path has also been suggested by many authors.<sup>20–22)</sup>

The formation of carbon dioxide through a catalytic oxidation of carbon monoxide is of significant practical importance, particularly in connection with pollution problems. Thus, one must also consider the fact that although recently a wide variety of theoretical techniques such as EHT (extended Hückel theory),<sup>23–25)</sup> CNDO,<sup>26–33)</sup> DV (discrete variational)-X $\alpha$ -SCF,<sup>34–37)</sup> LCMTO (linear combination of muffin-tin orbital),<sup>38,39)</sup> Localized orbital approach<sup>40,41)</sup> and *ab initio*<sup>42–44)</sup> have been applied for studying complex phenomenon on solid surfaces, most of these were aimed at obtaining a clear understanding of the chemisorption process in which the chemical reaction could be well described by the splitting of one bond and the formation of other bonds. The changes in various bond energies may, therefore, throw some interesting light on the disruption (weakening) and formation of various bonds; hence, the CNDO method as described here might become a good technique for studying simple reactions on metal surfaces, particularly since the bond energy is explicitly defined within its framework.

<sup>†</sup> Permanent address: Chemistry Department, University of Allahabad, Allahabad, India.

<sup>††</sup> Present address: National Chemical Laboratory for Industry, Yatabe, Ibaraki 305.

### Method of Calculation

Semiempirical methods like CNDO are flexible and convenient because of their inherent parametrized treatment; however, the involvement of many parameters makes them somewhat tedious and of lesser importance for systems containing transition metals. In the present paper the local core matrix elements  $U$ 's have been estimated from atomic data using the following expressions:

$$U_{ii} = -I_p(i) - (N-1)\gamma_{ss} - M\gamma_{sd} \quad (i=s \text{ or } p)$$

and

$$U_{dd} = -I_p(d) - (M-1)\gamma_{dd} - N\gamma_{sd}.$$

Here,  $I_p$  is the valence-state ionization potential,  $N$  denotes the total number of electrons in the valence "s" and "p" orbitals and  $M$  represents the number of electrons in "d" orbitals. The  $I_p$ 's have been calculated by using the method of Anno and Sakai,<sup>45</sup> where the valence orbital ionization potential (VOIP) was calculated with the help of the quadratic equation,

$$\text{VOIP} = A_0 + A_1Z + A_2Z^2. \quad (7)$$

Here,  $Z$  is the atomic number.  $A_0$  and  $A_1$  were evaluated with the help of

$$A_0 = a_0 + a_1M + a_2M^2 \quad (8)$$

and

$$A_1 = b_0 + b_1M. \quad (9)$$

The values of  $a_0$ ,  $a_1$ ,  $a_2$ ,  $b_0$ , and  $b_1$  were taken from Ref. 45. The exchange integral  $H_{ij}$  were calculated with the help of the Wolfsberg-Helmholtz approximation:<sup>46</sup>

$$H_{ij} = KS_{ij} (H_{ii} + H_{jj})/2. \quad (10)$$

An electronic configuration of  $3d^4 4s^4$  was assumed for the ground state of the Ni atom. Veigele<sup>47</sup> orbital exponents were used for Ni and Slater values were used for C and O. Thus, in the present calculation only  $K$  ( $=1.50$ ) was empirically chosen. The total energy was calculated from

$$E_t = 1/2 \sum_{r,s} P_{rs} (H_{rs} + F_{rs}) + \sum_{A<B} Z_A Z_B R_{AB}. \quad (11)$$

The bond energies between atoms A and B have been evaluated by the following equation:

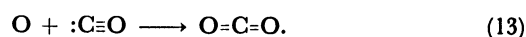
$$E_{AB} = \sum_r^A \sum_s^B (2P_{rs}\beta_{rs} - 1/2P_{rs}^2\gamma_{AB}) + (Z_A Z_B R_{AB}^{-1} - P_{AA}V_{AB} - P_{BB}V_{BA} + P_{AA}P_{BB}\gamma_{AB}). \quad (12)$$

In the above equations  $P_{rs}$  represents the density matrix,  $Z_A$  and  $Z_B$  represent the charge on nucleus A and B, respectively,  $V$  terms represent the potential integrals,  $R_{AB}$  represents the internuclear separation,

$\beta_{rs}$  is the resonance integral and  $\gamma_{AB}$  represents interelectronic repulsion between any electron on atom A and any electron on atom B.

### Results and Discussion

**1. Reaction of Carbon Monoxide and Oxygen Atom.** The aim of this section is to at least show the qualitative utility of the present method when it is applied to study a simple chemical reaction. The reaction of an oxygen atom with carbon monoxide has been studied in detail with the frontier orbital concept and is known to proceed as



This reaction should cause a strong stabilization in the energy of the  $3\sigma$  orbital of CO. In fact, the photoelectron spectra of CO and CO<sub>2</sub> show that the first  $\sigma$  orbital of CO<sub>2</sub> ionizes at 18 eV, whereas the  $3\sigma$  of CO ionizes at 14 eV,<sup>48</sup> consequently, the  $3\sigma$  of CO is stabilized by about 4 eV. In the present calculations the ionization potential for the first  $\sigma$  orbital of CO<sub>2</sub> was found to be 17.9 eV and the energy of the  $3\sigma$  orbital for CO came out to be 13.25 eV, which gives a stabilization energy of about 4.6 eV. This is in fairly good agreement with the experimental results.

The C-O<sub>a</sub> ("a" denotes the oxygen atom of CO) bond length was assumed to have a fixed value of 1.15 or 1.19 Å and the approaching oxygen atom O<sub>b</sub> was

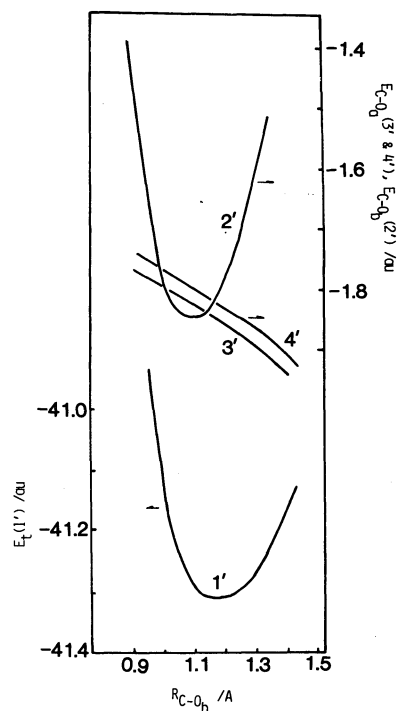


Fig. 1. Evaluation of total energy ( $E_t$ ) at  $R_{C-O_a} = 1.15$  Å and bond energies ( $E_{C-O}$ ) as a function of the bond length,  $R_{C-O}$  at fixed bond lengths of C-O<sub>a</sub>. 1':  $E_t$ , 2':  $E_{C-O_b}$ , 3':  $E_{C-O_a}$  at  $R_{C-O_a} = 1.15$  Å and 4':  $E_{C-O_a}$  at  $R_{C-O_a} = 1.19$  Å.

considered to exist along a linear path for calculating the total energy  $E_t$ , the bond energy of the C-O<sub>b</sub> bond (the new bond being formed, i.e.  $E_{C-O_b}$ ) and the bond energy of the C-O<sub>a</sub> bond (i.e.  $E_{C-O_a}$ ).

Figure 1 contains plots of  $E_t$ ,  $E_{C-O_b}$ , and  $E_{C-O_a}$  against  $R_{C-O_b}$  (the distance between C and O<sub>b</sub>). The total-energy curve 1' shows a minimum at 1.18 Å whereas the bond-energy curve 2' has a minimum at 1.13 Å. Both of these equilibrium distances are in fairly good agreement with the experimental bond length 1.16 Å for CO<sub>2</sub>.

The reaction path to form the CO<sub>2</sub> product (i.e. the formation of a new bond C-O<sub>b</sub>) is clearly depicted by curve 2'; however, curves 3' or 4' represent a weakening of the C-O<sub>a</sub> bond due to the approaching O<sub>b</sub>. This is caused by a delocalization of p<sub>z</sub> electrons of the approaching oxygen atom into the LUMO of CO, resulting in a simultaneous strengthening of the C-O<sub>b</sub> bond. It should be mentioned here that even for a different value of the C-O bond length (1.19 Å), the curves for the total energy  $E_t$  and the bond energy  $E_{C-O_b}$  were found to be almost identical and showed very little change. However, as expected, curve 4' for  $E_{C-O_a}$  is slightly different but runs almost parallel to the earlier curve 3'. This makes it clear that even if the bond length in CO is held constant, the curves representing the changes in various bond energies are capable of showing a weakening of the C-O<sub>a</sub> bond as well as the formation of a new bond between C and the approaching O atom.

Studies on this simple reaction have shown both qualitatively and quantitatively satisfactory results and have also made it very clear that the bond energy not only follows the pattern of the total energy of the system, but is also capable of depicting the weakening as well as the strengthening of various bonds.

In the next section the present method is applied to the CO oxidation on two types of clusters of nickel containing two and five atoms, respectively. Throughout this paper a value of 2.50 Å is used for the Ni-Ni distance (the same as that in bulk Ni) and 1.15 Å for the bond length of a CO molecule.

**2. Oxidation of CO on Ni<sub>2</sub> Cluster.** For Ni<sub>2</sub>, two different positions were considered for the preadsorbed O, namely: SYMMETRICAL and UNSYMMETRICAL. As shown in Fig. 2, in the first case two different sites were chosen for the coadsorption of CO (labeled as ON TOP (Model 1) and ADJACENT VERTICAL (Model 4)). However, in addition to the perpendicular models a slightly angular ( $\phi=30^\circ$ ) approach of CO (labeled as ADJACENT BENT (Model 3)) was included in the calculations. In the second case, the three similar types were also considered (Models 2, 5, 6). CO was supposed to be ON TOP (Model 2); an ADJACENT VERTICAL (Model 5) and an angular approach were also considered ( $\phi=30^\circ$ , Model 6). In the models 5 and 6, CO was supposed to be on top of

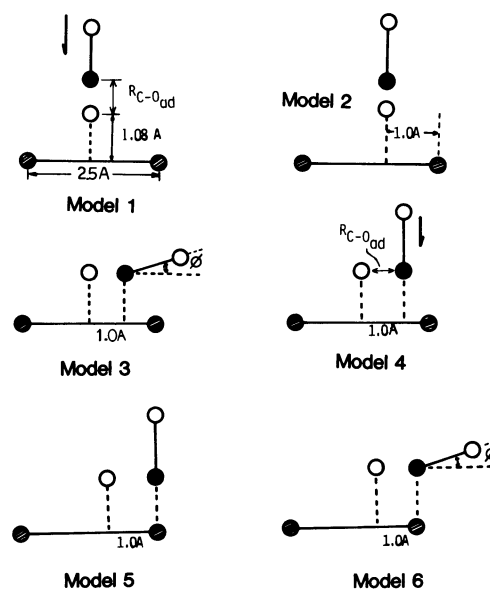


Fig. 2. Models for Ni<sub>2</sub>-O<sub>ad</sub> and Ni<sub>2</sub>-O-CO. 1: Symmetrical on top, 2: Unsymmetrical on top, 3: Symmetrical adjacent bent, 4: Symmetrical adjacent vertical, 5: Unsymmetrical adjacent vertical and 6: Unsymmetrical adjacent bent. ●: C, ●: Ni and ○: O atoms.

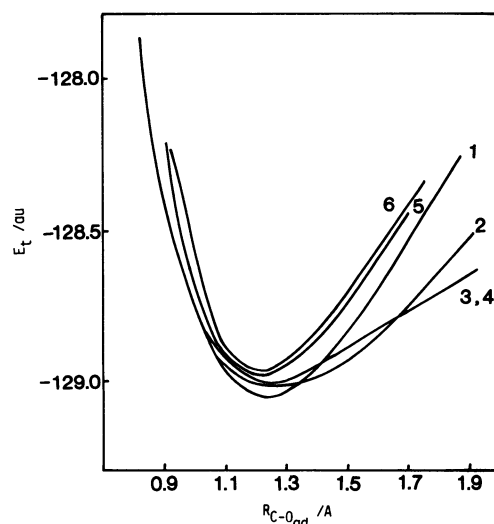


Fig. 3. Plots of  $E_t$  vs.  $R_{C-O_{ad}}$ . Notations of curves correspond to the numbers of models in Fig. 2.

one Ni atom, which models arise from the conclusion by Li and Tong by analysis of the LEED patterns of CO adsorption on Ni(100) surface.<sup>49</sup>

A plot of the total energy of the system  $E_t$  as a function of  $R_{C-O_{ad}}$  is given in Fig. 3; it can be said that the total energy of the system remains almost the same for all the models under study.

Figure 4 contains plots of  $E_{C-O_{ad}}$  as a function of  $R_{C-O_{ad}}$  and a comparative study of the various curves shows that for the bond formation between C and O<sub>ad</sub> three favourable arrangements are:

- (1) O preadsorbed symmetrically and CO on top,
- (2) O preadsorbed at an unsymmetrical site with CO lying on top,
- and
- (3) O preadsorbed symmetrically and CO adsorbed at an adjacent site in a bent form ( $\phi=30^\circ$ ). An increase or

decrease in this angle by  $10-15^\circ$  was found to have an adverse effect on bond formation.

Figure 5 shows the plots of the total bond energies between two Ni atoms and  $O_{ad}$ :  $\Sigma E_{Ni-O_{ad}}$  against  $R_{C-O_{ad}}$ . All of the curves shown here clearly indicate a weakening of the Ni- $O_{ad}$  bond, one of the requirements for the formation of a catalytic cycle. However, evidently this weakening is a maximum when O is symmetrically adsorbed and CO is adsorbed at an adjacent site in a bent form; the next best choice seems to be a symmetrical site for preadsorbed O with CO lying on top of it.

Plots of  $\Sigma E_{Ni-C}$  vs.  $R_{C-O_{ad}}$  are given in Fig. 6. It can be inferred from the nature of the various curves that CO may be attacking from the gas phase when it lies on top of either symmetrically or unsymmetrically adsorbed O; in other cases it seems to be adsorbed rather strongly.

In order to evaluate the possibility of a desorption of  $CO_2$ , the total energy of all the Ni- $O_{ad}$  and Ni-C bonds has been plotted against  $R_{C-O_{ad}}$  (Fig. 7) and the nature of the curves suggests that the desorption of  $CO_2$  should be easiest when O is symmetrically preadsorbed and CO lies on top of it, followed by unsymmetrical-on-top and symmetrical-adjacent-bent models.

**3. Oxidation of CO on  $Ni_5$  Cluster.** The  $Ni_5$  cluster model contains four atoms in the first layer; the fifth atom lies below in the second plane (Fig. 8). In all the cases, oxygen was supposed to be preadsorbed at a multi-center symmetrical site which lies on top of

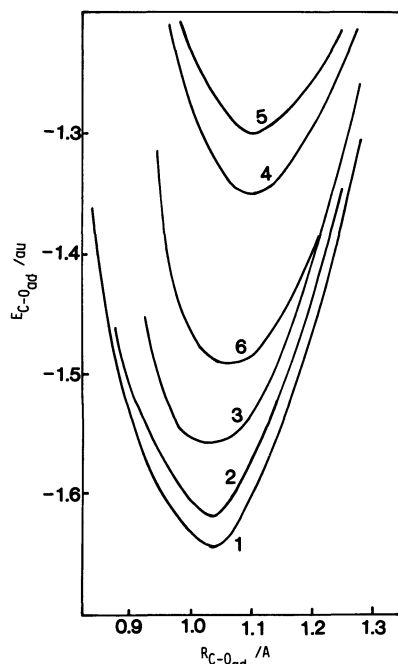


Fig. 4. Plots of  $E_{C-O_{ad}}$  vs.  $R_{C-O_{ad}}$ . Notations of curves correspond to the numbers of models in Fig. 2.

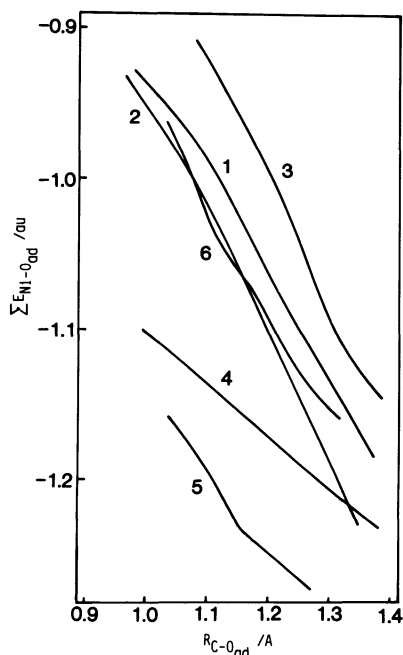


Fig. 5. Plots of  $\Sigma E_{Ni-O_{ad}}$  vs.  $R_{C-O_{ad}}$ . Notations of curves correspond to the numbers of models in Fig. 2.

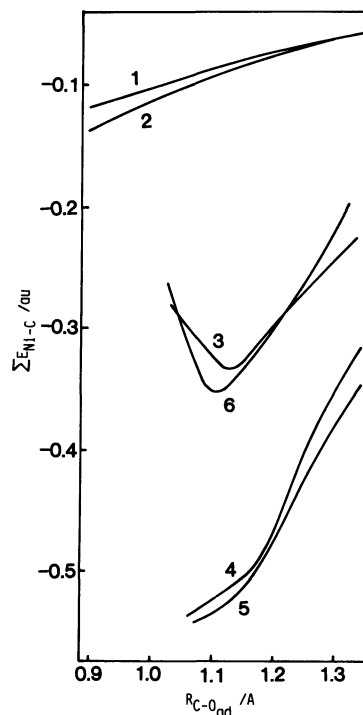


Fig. 6. Plots of  $E_{Ni-C}$  vs.  $R_{C-O_{ad}}$ . Notations of curves correspond to the numbers of models in Fig. 2.

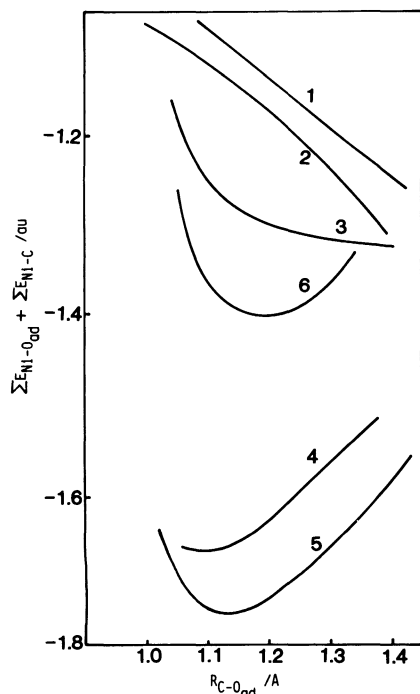


Fig. 7. Plots of  $\sum E_{Ni-C} + \sum E_{Ni-O_{ad}}$  vs.  $R_{C-O_{ad}}$ . Notations of curves correspond to the numbers of models in Fig. 2.

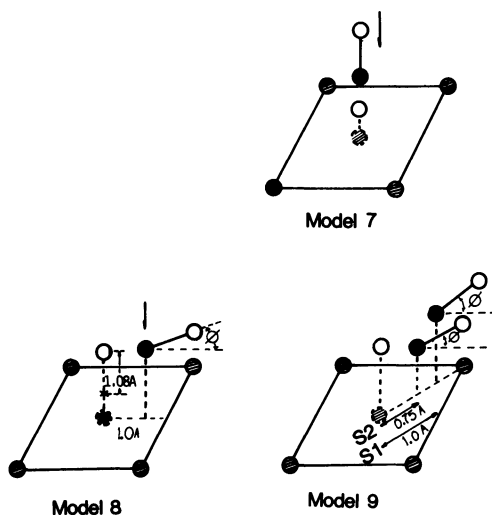


Fig. 8. Models for  $Ni_5$  cluster and  $Ni_5-O-CO$ . 7: On top, 8: on bridge, 9: on diagonal. Note that two different site labeled S1 and S2 for the model 9 are distinguished for the adsorption site of CO. ●: surface Ni, ○: second layer Ni, ●: C and ○: O atoms.

the fifth Ni atom. For CO, however, in addition to a site on top of  $O_{ad}$  (Model 7), two other sites were also chosen:

(a) CO adsorbed at an adjacent BRIDGE site as shown in Model 8. (b) CO adsorbed at a site on the DIAGONAL (Model 9). However, in this case in order to study the effect of the preadsorbed O on the adsorption of CO, two different sites were selected

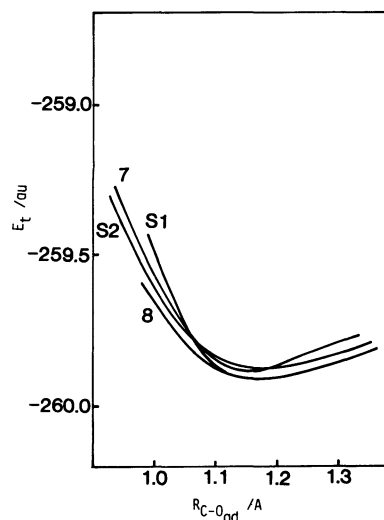


Fig. 9. Plots of  $E_t$  vs.  $R_{C-O_{ad}}$ . Curves 7,8, S1, and S2 correspond to models 7,8,9-S1 and 9-S2 in Fig. 8, respectively.

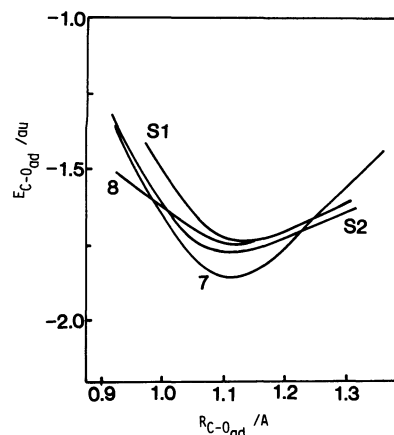


Fig. 10. Plots of  $E_{C-O_{ad}}$  vs.  $R_{C-O_{ad}}$ . Notations of curves are the same to those in Fig. 9.

which are denoted as S1 and S2, respectively, in Model 9. Relying on our previous experience with  $Ni_2$  where the bent approach was found to be more appropriate for the formation as well as desorption of  $CO_2$ , we decided to consider only the angular approach of CO for adsorption ( $\phi=30^\circ$ ).

Figure 9 shows plots of  $E_t$  as a function of  $R_{C-O_{ad}}$ , from which it becomes evident that the total energy of the system does not differ appreciably for different models.

Figure 10 contains different curves for a plot of  $E_{C-O_{ad}}$  as a function of  $R_{C-O_{ad}}$  and a comparative study suggests that an on-top site may be slightly more favourable for the formation of  $CO_2$ .

Figure 11 represents a plot of  $\sum E_{Ni-O_{ad}}$  against  $R_{C-O_{ad}}$ . Although no clear-cut observation can be made since in all the cases the Ni- $O_{ad}$  bond shows a tendency of becoming weaker with the approach of CO the DIAGONAL-S2 site for CO adsorption may be

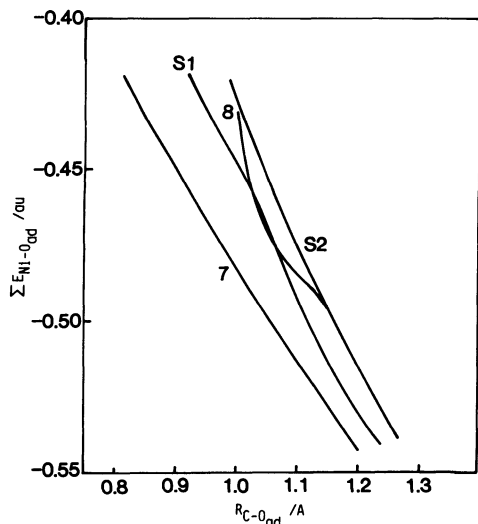


Fig. 11. Plots of  $\Sigma E_{\text{Ni-O}_{ad}}$  vs.  $R_{\text{C-O}_{ad}}$ .  
Notations of curves are the same to those in Fig. 9.

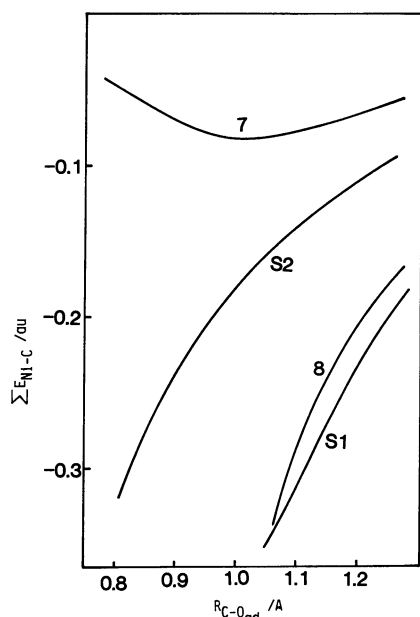


Fig. 12. Plots of  $\Sigma E_{\text{Ni-C}}$  vs.  $R_{\text{C-O}_{ad}}$ .  
Notations of curves are the same to those in Fig. 9.

slightly more favorable for such a weakening.

Figure 12 shows plots of  $\Sigma E_{\text{Ni-C}}$  against  $R_{\text{C-O}_{ad}}$ ; these curves show some interesting features regarding the adsorption of CO on Ni preadsorbed with O. A comparison of curves S1 and S2 shows that as CO moves closer to the preadsorbed O, the strength of Ni-C bond decreases considerably. The effect of preadsorbed electronegative atoms on the adsorption of CO and H<sub>2</sub> has been studied by Kiskinova<sup>50</sup> using thermal desorption, LEED and AES. It was found that the presence of electronegative atoms causes a reduction in the adsorption rate, the adsorption bond strength and the capacity of the Ni surface for CO and H<sub>2</sub> adsorption. The same conclusion was reached by Madix<sup>51</sup> for the case of iron. Our theoretical results

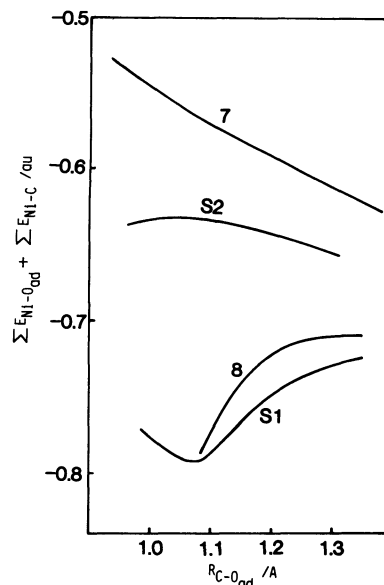


Fig. 13. Plots of  $\Sigma E_{\text{Ni-O}_{ad}} + \Sigma E_{\text{Ni-C}}$  vs.  $R_{\text{C-O}_{ad}}$ .  
Notations of curves are the same to those in Fig. 9.

are in agreement with these results, clearly indicating a predominant role for the preadsorbed O.

Figure 13 contains plots of the sum of  $\Sigma E_{\text{Ni-C}}$  and  $\Sigma E_{\text{Ni-O}_{ad}}$  against  $R_{\text{C-O}_{ad}}$ . On the basis of these curves it is suggested that ON BRIDGE and ON DIAGONAL-S1 which are comparatively far from the O<sub>ad</sub> may not be suitable for the desorption of CO<sub>2</sub>, which is otherwise known to desorb immediately from the surface at usual catalytic temperatures (>100°C<sup>52</sup>). The remaining two possibilities (namely ON TOP and ON DIAGONAL-S2) are, perhaps, good adsorption sites as far as the desorption of CO<sub>2</sub> is concerned. In order to evaluate the effect of neighbouring O<sub>ad</sub> atoms, it was considered appropriate to include four such nearest-neighbour O<sub>ad</sub> atoms in one calculation set for both on-top and on-diagonal sites. It was also found that the various bond energies remain almost unaffected, probably due to the large distance.

On the basis of the qualitative studies presented in this paper it is suggested that the reaction of CO and O<sub>2</sub> on nickel might consist of the following stages:

(1) **Preadsorption of Ni with Oxygen:** Engel et al.<sup>53</sup> have observed that the chemisorbed oxygen is the primary surface species formed by an interaction of O<sub>2</sub> with the surface of platinum metals and that this species generally exhibits a higher reactivity towards CO. They further suggest that as long as the actual concentration of oxygen under a steady-state condition is low it may be safely concluded that if the temperature is not extremely high the chemisorbed atomic oxygen is the only species that enters into the catalytic oxidation of CO. Our studies of Ni<sub>2</sub> clusters suggest that the symmetrical site is more suitable both for the formation and desorption of CO<sub>2</sub>; this is in agreement with the findings based upon LEED

studies.

(2) **Oxidation of Carbon Monoxide at Low Coverage of Oxygen:** It has been concluded by Engel<sup>53)</sup> that if both kinds of particles (i.e. CO and O) are present on the surface, the CO can be regarded as moving within an essentially fixed matrix of O<sub>ad</sub> atoms. On the basis of the present studies regarding both Ni<sub>2</sub> and Ni<sub>5</sub>, it is suggested that at a low coverage of oxygen, CO might be adsorbed at an adjacent site and that in the transition state this adsorbed mobile species assumes a bent configuration which has been found to be more favorable for the formation (as well as desorption) of CO<sub>2</sub>. The possibility of an angular form of adsorbed CO in the transition state has also been suggested by Anderson<sup>54)</sup> while describing the mechanism of CO oxidation on Pt. Obviously, the oxidation of CO at low coverage of oxygen can be assumed to follow the Langmuir-Hinshelwood path.

(3) **Oxidation of Carbon Monoxide at High Coverage of Oxygen:** Behm et al.<sup>55)</sup> have noted that for a reaction of preadsorbed oxygen during exposure to CO on Pt(100) at 355 K and at pressures upto  $1 \times 10^{-4}$  Pa the CO coverage is negligibly small as long as  $\theta_0 > 0.05$ . With respect to the relative rates of adsorption, reaction and desorption, this means that the latter two processes must be at least as fast as CO adsorption. It has also been found that the lifetime of a chemisorbed CO adjacent to a chemisorbed O on Pt is  $\approx 10^{-4}$  s. It has reaction probability of unity for each chemisorbed CO; however, at a high coverage of O<sub>ad</sub> or in the case of CO<sub>ad</sub> exposed to O<sub>2</sub>, the CO<sub>ad</sub> is held by a matrix of surrounding oxygen atoms and such islands of the two species can coexist on the surface for hundreds of seconds with very little reaction probability for CO<sub>2</sub> formation. The theoretical results on Ni<sub>2</sub> and Ni<sub>5</sub> in the present paper suggest that under such conditions there is a high probability of a reaction between adsorbed oxygen and CO from the gas phase following an Eley-Rideal type mechanism including a "precursor state."

One of the authors (A. K. S.) would like to express sincere thanks to Ministry of Education, Japan and UNESCO for being awarded a fellowship. Thanks are also due to Dr. K. Shimokoshi for his help in computations and his fruitful discussions. The computations were performed at the computer center of Tokyo Institute of Technology, as well as the Institute for Molecular Science at Okazaki.

#### References

- 1) G. Ertl and P. Rau, *Surface Sci.*, **15**, 443 (1969).
- 2) H. Conrad, G. Ertl, and G. K ppers, *Surface Sci.*, **76**, 323 (1978).
- 3) G. Ertl and J. Koch, *Z. Phys. Chem.*, **69**, 323, (1970).
- 4) G. Ertl and J. Koch, "Adsorption Desorption Phenomenon," Academic Press N. Y. (1972).
- 5) G. Ertl and J. Koch, "Proceeding of 5th Intern. Congr. Catalysis, Florida (1972)," p. 969.
- 6) G. Ertl and Neumann, *Z. Phys. Chem.*, **90**, 127 (1974).
- 7) T. Engel and G. Ertl, *Chem. Phys. Lett.*, **54**, 95 (1978).
- 8) T. Engel and G. Ertl, *J. Chem. Phys.*, **69**, 1267 (1978).
- 9) A. M. Horgan and D. A. King, *Trans. Farad. Soc.*, **67**, 2145 (1971).
- 10) T. H. Lindstrom and T. T. Tsotsis, *Surface Sci.*, **150**, 487 (1985).
- 11) T. H. Lindstrom and T. T. Tsotsis, *Surface Sci.*, **147**, 647 (1984).
- 12) J. S. Close and J. M. White, *J. Catal.*, **36**, 185 (1975).
- 13) T. Matsushima and J. M. White, *J. Catal.*, **39**, 265 (1975).
- 14) T. Matsushima, D. B. Almy, D. C. Foyt, J. S. Close, and J. M. White, *J. Catal.*, **39**, 277 (1975).
- 15) T. Matsushima, D. B. Almy, D. C. Foyt, J. S. Close, and J. M. White, *J. Catal.*, **40**, 334 (1975).
- 16) T. Matsushima, D. B. Almy, D. C. Foyt, J. S. Close, and J. M. White, *J. Catal.*, **41**, 397 (1976).
- 17) M. Wulf and P. T. Dawson, *Surface Sci.*, **65**, 399 (1975).
- 18) J. K ppers and A. Plagge, *J. Vacuum Sci. Technol.*, **13**, 259 (1976).
- 19) J. W. Davenport, *Phys. Rev. Lett.*, **36**, 945 (1976).
- 20) J. Harris and .Kasemo, *Surface Sci.*, **105**, L281 (1981).
- 21) J. Harris and B. Kasemo, *Surface Sci.*, **105**, L288 (1981).
- 22) E. G. Keim, F. Labohm, O. L. J. Gizeman, G. A. Bootsma, and J. W. Geus, *Surface Sci.*, **112**, 52 (1981).
- 23) R. C. Baetzold, *Inorg. Chem.*, **20**, 52 (1981).
- 24) R. C. Baetzold, M. G. Mason, and J. F. Hamilton, *J. Chem. Phys.*, **72**, 366 (1980).
- 25) R. C. Baetzold, *Advan. Catal.*, **25**, 1 (1976).
- 26) G. Blyholder, *J. Chem. Soc., Chem. Commun.*, **1973**, 625.
- 27) G. Blyholder, *J. Chem. Phys.*, **62**, 3193 (1975).
- 28) G. Blyholder, *J. Phys. Chem.*, **79**, 756 (1975).
- 29) G. Blyholder, *J. Vacuum Sci. Technol.*, **11**, 865 (1974).
- 30) G. Blyholder, *Surface Sci.*, **42**, 249 (1974).
- 31) H. Kobayashi, H. Kato, K. Tarama, and F. Fukui, *J. Catal.*, **49**, 294 (1977).
- 32) J. Spanget-Larsen, *Theoret. Chim. Acta*, **55**, 165 (1980).
- 33) R. C. Baetzold, *J. Chem. Phys.*, **68**, 555 (1978).
- 34) E. Miyazaki, M. Tsukada, and H. Adachi, *Surface Sci.*, **131**, L390 (1983).
- 35) K. H. Johnson, *Ann. Rev. Phys. Chem.*, **26**, 39 (1975).
- 36) D. R. Salahub and R. P. Messermer, *Phys. Rev.*, **B16**, 2526 (1977).
- 37) G. Seifert, E. Mrosan, and H. Mueller, *Phys. Status Solidi*, **B89**, 553 (1978).
- 38) R. V. Kasowski, *Surface Sci.*, **63**, 370 (1977).
- 39) R. V. Kasowski and E. Caruthers, *Phys. Rev.*, **B21**, 3200 (1980).
- 40) D. W. Bullett, *Surface Sci.*, **68**, 149 (1977).
- 41) D. W. Bullett and E. P. O. Reilly, *Surface Sci.*, **89**, 274 (1979).
- 42) H. Stoll and H. Preuss, *Phys. Status Solidi*, **B64**, 103 (1974).
- 43) C. W. Bauschlicher, P. S. Bagus, and H. F. Schaefer, *I. B. M. J. Res. Develop.*, **22**, 213 (1978).
- 44) C. F. Melius, T. H. Upton, and W. A. Goddard, (III), *Solid. State. Commun.*, **28**, 501 (1978).
- 45) T. Anno and. Y. Sakai, *Theoret. Chim. Acta*, **18**, 208 (1970).

- 46) M. Wolfsberg and C. Helmholtz, *J. Chem. Phys.*, **20**, 837 (1952).
- 47) W. J. Veigle, D. E. Stevenson, and E. M. Henry, *J. Chem. Phys.*, **50**, 208, (1969).
- 48) R. L. DeKock and H. B. Gray, *Chemical Structure and Bonding*, Benjamin Inc., (California (1980)). p. 321.
- 49) C. H. Li, S. Y. Tong, *Phys. Rev. Lett.*, **43**, 360 (1979).
- 50) M. Kisikina and D. W. Goodman, *Surface Sci.*, **108**, 64 (1981).
- 51) J. Benziger and R. J. Madix, *Surface Sci.*, **94**, 119 (1980).
- 52) T. Engel and G. Ertl, "The Chemical Physics of Solid Surfaces and Heterogeneous Catalysis," Elsevier, N. Y. (1982), Vol. 4, p. 78.
- 53) T. Engel and G. Ertl, *Adv. Catal.* **28**, 1 (1979).
- 54) N. K. Rya and A. B. Anderson, *Surface Sci.*, **119**, 35 (1982).
- 55) R. J. Behm, P. A. Thiel, P. R. Norton, and P. E. Binder, *Surface Sci.*, **147**, 143 (1984).
-